ELSEVIER

Materials Science and Engineering A233 (1997) 103–110

MATERIALS SCIENCE & ENGINEERING A

The plasticity of icosahedral quasicrystals

M. Feuerbacher [a,*], C. Metzmacher [a], M. Wollgarten [a], K. Urban [a], B. Baufeld [b], M. Bartsch [b], U. Messerschmidt [b]

[a] *Institut für Festkörperforschung, Forschungszentrum Jülich GmbH, D-52425 Jülich, Germany*
[b] *Max-Planck-Institut für Mikrostrukturphysik, D-06120 Halle/Saale, Germany*

Received 11 September 1996; received in revised form 3 December 1996

Abstract

The experimental aspects of the plastic deformation of icosahedral quasicrystals are reviewed. Macroscopic experiments, which involve the general investigation of stress–strain curves and the determination of the thermodynamic activation parameters of the deformation process are described. Investigations of the microstructure of plastically deformed samples, studied by means of transmission electron microscopy are presented. Important parameters such as the dislocation density, the Burgers vectors of dislocations, and slip systems are analyzed. Additionally, the results of in-situ straining experiments giving direct insight into the dynamics of the deformation process are presented. Direct conclusions on the nature of the plastic deformation process are drawn, and the current view of the deformation mechanism based on the specific structure of this class of materials is consistently discussed in terms of a qualitative 'cluster friction model'. © 1997 Elsevier Science S.A.

Keywords: Icosahedral quasicrystals; Plastic deformation; Transmission electron microscopy

1. Introduction

Quasicrystals represent a new state of solid matter exhibiting orientational but no translational order. Their diffraction patterns show sharp Bragg peaks revealing symmetries incompatible with periodicity, and they cannot be indexed to any Bravais lattice.

The first quasicrystalline phase was discovered in 1984 by Shechtman et al. [1] in a rapidly quenched Al–Mn alloy. It exhibits an icosahedral point group symmetry involving 5-fold axes and is therefore called icosahedral quasicrystal[1]. Subsequently, further quasicrystalline phases were found in other binary alloys, but they all were metastable and intrinsically defective. The first thermodynamically stable quasicrystal was found in the Al–Li–Cu system [2] in 1986. However, this phase still showed a high degree of disorder. With the discovery of Al–Cu–Fe [3] in 1988 the era of 'perfect quasicrystals' began. These are stable and show undistorted diffraction patterns with peak widths only limited by the instrument resolution, corresponding to a very high degree of structural and chemical order. Icosahedral Al–Pd–Mn [4] was the first (and so far the only) phase in which single-quasicrystals can be grown by the Czochralski technique [5,6]. This allows for the production of single-quasicrystals several centimeters in size, exhibiting a very high structural quality.

The mechanical properties of these new materials have been the subject of numerous studies since the early days of quasicrystals. Measurements of the hardness and the elastic properties were performed on some poly-quasicrystalline alloys [7,8], Al–Li–Cu single-grains [9], decagonal Al–Cu–Co–Si single-quasicrystals [10] and on icosahedral Al–Pd–Mn single-quasicrystals [11,12]. The anelastic properties of single-quasicrystalline icosahedral Al–Pd–Mn were determined by Feuerbacher et al. [13].

Quasicrystals are brittle at room temperature, but at elevated temperatures they show extensive ductility. Plastic deformation experiments in the high-temperature range were firstly performed on poly-quasicrystalline alloys [14–17]. The first stress–strain curves of

* Corresponding author.

[1] Other classes of quasicrystals, showing 8-fold, 10-fold, or 12-fold rotational axes are called octagonal, decagonal or dodecagonal quasicrystals, respectively. However, in this paper the emphasis will be laid on icosahedral quasicrystals.

PII S0921-5093(97)00053-1

Al–Pd–Mn single-quasicrystals were recorded by Yokoyama et al. [11]. Wollgarten et al. [18] found evidence for the existence of a dislocation mechanism in the plastic deformation of icosahedral quasicrystals. The intrinsic thermodynamic activation parameters of the plastic deformation process were determined by Feuerbacher et al. [19]. Rosenfeld et al. [20] studied the microstructure of deformed Al–Pd–Mn single-quasicrystals. High-temperature in-situ straining experiments, which gave the first direct evidence of dislocation motion in quasicrystals, were performed by Wollgarten et al. [21]. Dislocation motion in quasicrystals was also investigated theoretically in analytical studies [22] and by molecular dynamic simulations in a two-dimensional binary tiling [23,24].

In this paper, a review is given of experiments on the plastic behavior of icosahedral quasicrystals. For this purpose, we first give a brief introduction to defects in quasicrystals, with the emphasis on dislocations and phasons, which are both closely connected to the plastic deformation process. Three experimental approaches for the investigation of the plasticity of these materials are described and illustrated by experiments on icosahedral Al–Pd–Mn single-quasicrystals. These are macroscopic straining experiments, microstructural investigations of plastically deformed material in a transmission electron microscope (TEM) and in-situ straining experiments. The simultaneous interpretation of all experimental results leads to a consistent picture of the plastic deformation process, reflecting the current understanding of the deformation mechanism in icosahedral quasicrystals.

2. Defects in quasicrystals

2.1. Construction of an ideal quasicrystal

Due to the lack of translational symmetry, a quasicrystal cannot be constructed, as a crystal, by periodic continuation of an elementary unit cell. The current deterministic models [25,26] for the construction of a quasicrystal describe the quasiperiodic structure through a projection formalism using a higher-dimensional periodic lattice, the so-called hyperlattice [27]. The icosahedral quasicrystal is constructed by reference to a six-dimensional hypercubic lattice. This hyperlattice is embedded in a six-dimensional reference space, which can be divided into two three-dimensional, orthogonal subspaces, one of which is the real, physical space $E_\parallel$. The other subspace, consisting of the remaining three dimensions, is called perpendicular space $E_\perp$. In six-dimensional space, a unit cell is defined and decorated with hyperatoms having only an extension in perpendicular space $E_\perp$. The cuts of the hyperatoms with the subspace $E_\parallel$ define the atomic positions in physical space, i.e., the structure of the ideal quasicrystal. This representation of the quasicrystal structure by high-dimensional crystallography (cut technique) has the advantage that many concepts known from solid-state physics can be adapted to quasicrystals by extension to hyperspace. This is for example the case for the construction and analysis of dislocations in quasicrystals.

The cut technique is equivalent to a unit cell representation, which describes the structure of the quasicrystal as a suitable decoration of a quasiperiodic arrangement of at least two building blocks. These are arranged according to strict matching rules. An icosahedral quasicrystal can be constructed in this way by the use of two elementary tiles, a thick and a flat rhombohedron. Because of the matching rules, the resulting ideal quasicrystal is fully deterministic and perfectly ordered.

2.2. Strain fields in icosahedral quasicrystals

A strain field in an icosahedral quasicrystal has to be described referring to six-dimensional hyperspace [28]. It can be introduced by displacing hyperatoms from positions $\vec{X}_0$ in six-dimensional space to positions $\vec{X}_1 = \vec{X}_0 + \vec{U}$, where $\vec{U}$ is a six-dimensional displacement vector. Consequently, strain fields have components in both the physical and perpendicular subspace $\vec{U} = \vec{u}_\parallel + \vec{u}_\perp$. The physical space component $\vec{u}_\parallel$ describes strain components parallel to directions in $E_\parallel$, which means that relative translations of atoms in physical space occur. This is in complete analogy to strains in conventional crystalline materials and is therefore called *phonon strain*. The orthogonal space part $\vec{u}_\perp$ describes translations of the hyperatoms in $E_\perp$, that is perpendicular to the cut space $E_\parallel$. Thus, under the influence of the strain field, some cuts of hyperatoms with $E_\parallel$ disappear while others, at different positions, emerge[2]. This leads to *discrete* atomic displacements in physical space. In the unit cell representation, the corresponding defects cause violations of the matching rules [29] and thus, give rise to structural and chemical disorder in physical space. These defects cannot occur in conventional crystalline materials and are referred to as *phason defects* or *phasons*.

2.3. Dislocations in icosahedral quasicrystals

Dislocations in icosahedral quasicrystals are treated in six-dimensional hyperspace analogously to crystal dislocations in three dimensions [30,31]. For example, a hyperlattice edge dislocation can be constructed per-

[2] The extensions of the hyperatoms have to be chosen in such a way that the number of atoms in physical space is constant (closeness condition [32]).

forming a generalized Volterra process where a five-dimensional halfplane is introduced into the hyperlattice. The six-dimensional strain field $\vec{U}$ corresponding to the quasicrystal dislocation is related to the six-dimensional Burgers vector $\vec{B}$ via a Burgers circuit C by

$$\vec{B} = \oint_C \mathrm{d}\vec{U} \tag{1}$$

Thus, the six-dimensional Burgers vector has components in both subspaces,

$$\vec{B} = \vec{b}_{\parallel} + \vec{b}_{\perp} \tag{2}$$

i.e., the phonon part $\vec{b}_{\parallel}$ in physical space and the phason part $\vec{b}_{\perp}$ in orthogonal space. The corresponding strain fields cause phonon and phason strain, respectively, in physical space. The phonon part of the Burgers vector has the same meaning as a Burgers vector in crystals, i.e., it describes the dislocation strain field and it acts as an elementary slip step in physical space. The modulus of the phason component is a measure of the number of phason defects associated with the dislocation.

Dislocations in quasicrystals can be classified according to their Burgers vector direction in physical space and their *strain accommodation parameter* ζ. This quantity is defined as the ratio of the moduli of the phason and the phonon component of the Burgers vector

$$\zeta = |\vec{b}_{\perp}|/|\vec{b}_{\parallel}| \tag{3}$$

It describes how the dislocation elastic energy is distributed into phason and phonon parts. The parameter ζ can be represented in the form $\zeta = \tau^n$, where $\tau = (1 + \sqrt{5})/2$ is the number of the golden mean. For dislocations with Burgers vectors parallel to 2-fold quasilattice directions (in the following referred to as 2-fold Burgers vectors), the exponent n is always an odd integer whereas in the case of 5-fold or 3-fold Burgers vectors, n is even.

Since the strain field of a quasicrystal dislocation has not only phonon but also phason strain contributions, the techniques for dislocation analysis in crystals cannot be applied to quasicrystals. The determination of Burgers vectors in quasicrystals requires an extended contrast extinction technique [33] or defocus convergent beam electron diffraction technique (d-CBED) [34]. The latter allows for the determination of all six components of the quasicrystal dislocation Burgers vector and was applied for the dislocation analysis presented in this paper.

3. Macroscopic deformation experiments

3.1. Experimental details

Specimens of $Al_{70.5}Pd_{21}Mn_{8.5}$ of $7 \times 2 \times 2$ mm^3 in size were cut from a Czochralski-grown single-quasicrystal by spark erosion. All edges were oriented parallel to 2-fold directions. The faces were carefully ground and polished. Samples were deformed in compression at temperatures between 680 and 800°C in an Instron 8562 testing system under closed-loop strain control mode at a constant strain rate of 10^{-5} s^{-1}. The activation volume and the stress exponent were determined by means of dynamic stress relaxation experiments and by strain rate changes (SRC). For the determination of the activation enthalpy, differential temperature changes in combination with stress relaxation experiments were performed. A detailed description of the procedure is given in Ref. [19]. The long-range internal stresses were determined by means of stress transient dip tests at 760°C.

The analysis of the experimental data is based on the thermodynamic formalism generally used for crystalline materials (for a review see Ref. [35]), which is adopted here for the investigation of the plastic behavior of quasicrystals.

3.2. Experimental results

Fig. 1 shows true-stress/true-strain curves at two different temperatures of 760 and 800°C. The most prominent feature of these curves is the complete absence of work hardening. After the yield drop, the stress continuously decreases with increasing strain. This is observed at all temperatures investigated. No saturation of this effect up to deformations of 20% was observed. Fig. 2 shows the temperature dependence of the yield stress σ_{max}. It decreases from about 750 Mpa at 680°C to 120 MPa at 800°C. The stress exponent decreases slightly from about 5.0 at 680°C to 3.5 at 800°C. The activation volume, plotted in Fig. 3, ranges from about 1.2 nm^3 at 120 MPa to 0.16 nm^3 at 740 MPa. For the calculation of V from the stress relaxation data, a

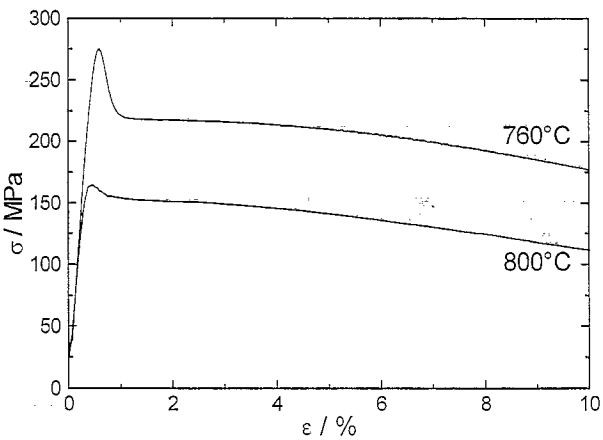

Fig. 1. Stress–strain curves of icosahedral Al–Pd–Mn at two different temperatures (760 and 800°C) and a strain rate of 10^{-5} s^{-1}.

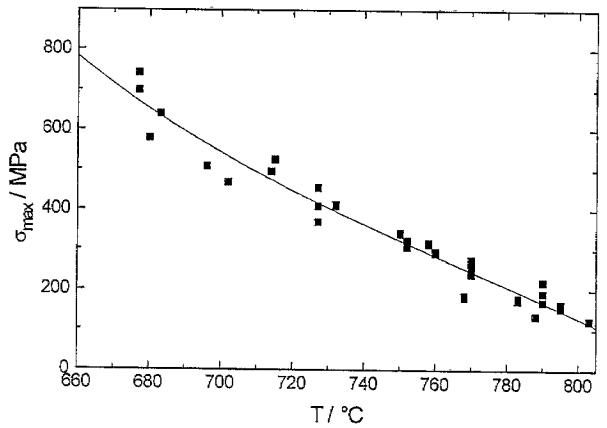

Fig. 2. Temperature dependence of the yield stress σ_{max}.

Schmid factor $m_S = 0.5$ was used because of the high structural isotropy of the material. The activation volume is about two orders of magnitude larger than $b_{\parallel}^3$, where $b_{\parallel}$ describes the modulus of the physical space component of the six-dimensional Burgers vector. The most frequently observed Burgers vector length $b_{\parallel} = 0.183$ nm (Section 4.2) was used for comparison. The stress dependence of V can be described by a hyperbolic function as a good approximation. The results obtained by SRC are included in the figure by open circles. They are in very good agreement with the values obtained by the stress relaxation experiments.

The dip tests yield internal stresses of about 60 MPa at 760°C, which is about 20% of the yield stress at this temperature.

The activation enthalpy was determined as 6.3 eV at 700°C, increasing to 7.4 eV at 800°C. Its temperature dependence is depicted in Fig. 4. The line is a linear fit to the data points with $\Delta H(T = 0\ \mathrm{K}) = 0$. The work term ΔW describes that part of the activation energy to be supplied by the applied stress. Its upper bound can be calculated by $\Delta W \approx \tau V$. This quantity is constant in

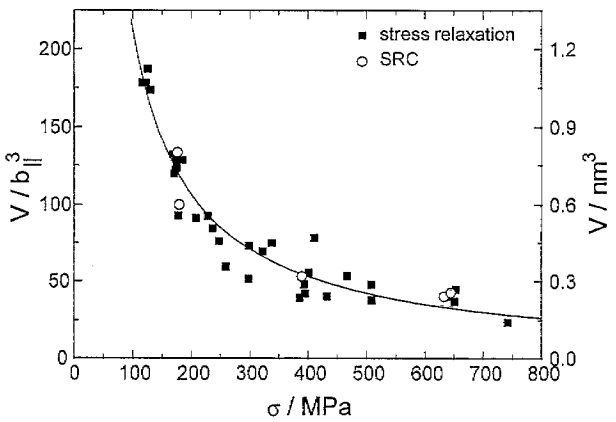

Fig. 3. Activation volume V vs. stress σ. The line is a hyperbolic fit to the data points.

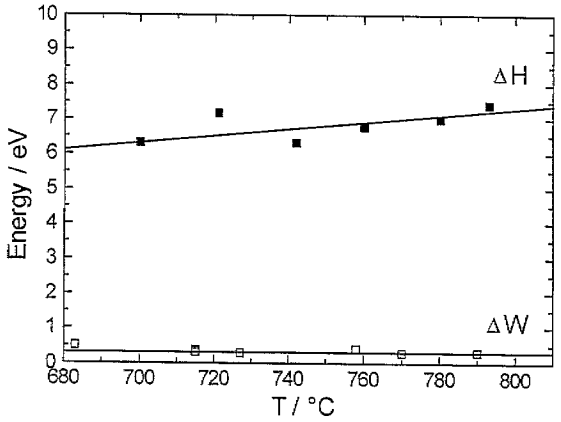

Fig. 4. Activation enthalpy ΔH and work term ΔW as a function of temperature.

the temperature range investigated and amounts to about 0.35 eV, which is considerably smaller than the value found for the activation enthalpy.

4. TEM investigations of deformed samples

4.1. Experimental procedure

After deformation, the samples were unloaded and quenched in water in order to store the actual defect structure. TEM specimens were prepared by standard techniques. Reference samples, which underwent the same temperature program as the deformed material, were prepared similarly. For a more detailed description of the procedure see Ref. [20]. The microscopic examinations were carried out in JEOL 4000FX and 2000EX electron microscopes operated at an acceleration voltage of 200 kV.

Dislocation densities in deformed and undeformed samples were determined by counting the penetration points of dislocation lines with the foil surfaces in large specimen areas. Burgers vectors were analyzed by d-CBED. The line directions of dislocation segments were determined by stereographic projection.

4.2. Experimental results

Fig. 5 shows a bright-field image of the dislocation arrangement in a sample deformed by 6% at 760°C. The foil normal of the specimen is parallel to a 5-fold [0/0 0/1 1/0] direction in the notation of Ref. [36]. The inspection of the electron diffraction images of deformed specimens shows that no phase transformation to a non-icosahedral phase has taken place.

The dependence of dislocation density ρ on plastic strain ε_p in samples deformed at 760°C is shown in Fig. 6(a). The data points correspond to different stages of

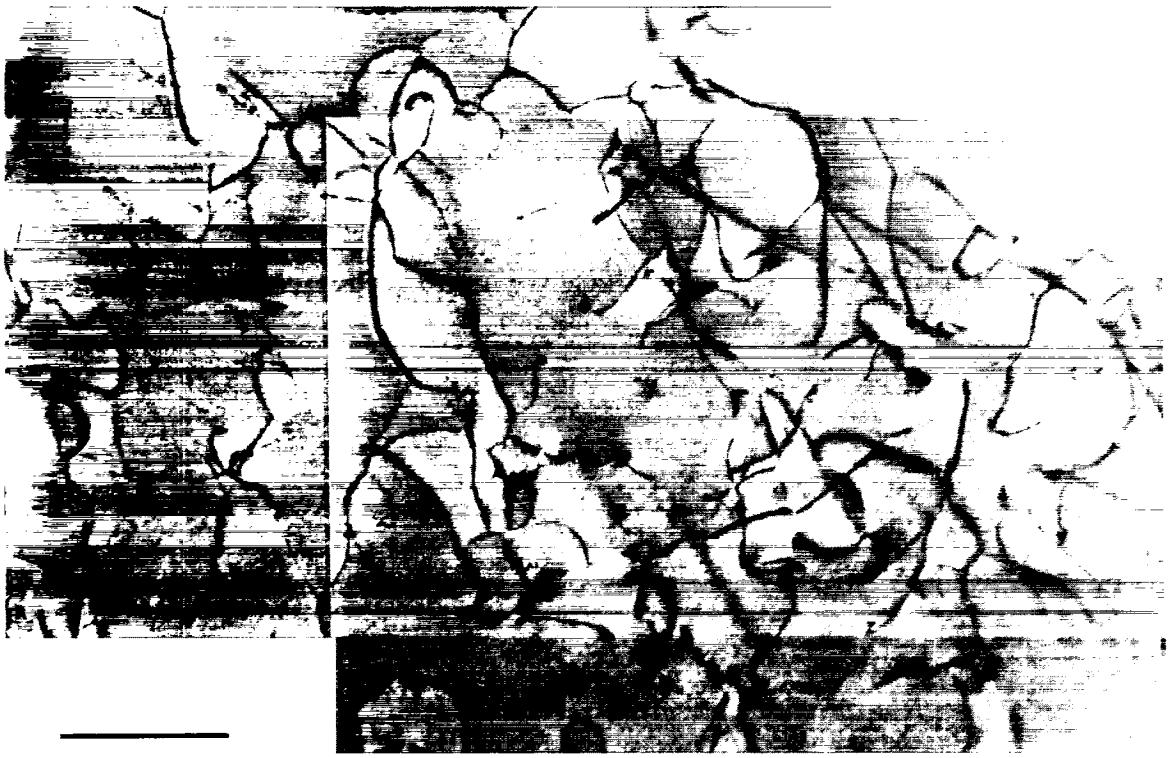

Fig. 5. Bright-field image of the dislocation arrangement in a sample deformed by 6% at 760°C. Bar = 1 μm.

plastic deformation marked by arrows in Fig. 6(b). The first point (0%) corresponds to the undeformed reference sample, the third (0.15%) to the upper yield point. The dislocation density increases significantly at the onset of plastic deformation. The yield drop in the stress–strain curve is accompanied by a strong dislocation multiplication. At high plastic strains, the dislocation density decreases significantly. The ratio of the dislocation density at 10% plastic strain and the maximum dislocation density amounts to 0.75. Similar behavior is observed at other deformation temperatures. However, the dislocation density decreases with increasing temperature [20].

More than 90% of the dislocations investigated in the deformed material are perfect dislocations and show 2-fold Burgers vectors. Less frequently, 5-fold (5%) and 3-fold (3%) Burgers vectors are found. All 5-fold, 3-fold and pseudo-2-fold Burgers vectors observed are no lattice vectors in hyperspace, i.e. the corresponding dislocations are partials.

The strain accommodation parameter ζ is always found to be larger than unity. Values ranging from $\tau^3 \approx 4.2$ to $\tau^8 \approx 47.0$ are found in deformed specimens. In Fig. 7(a), normalized distribution curves N_ζ of ζ-values of dislocations with 2-fold Burgers vectors are plotted. Each curve shows the distribution for a certain value of plastic strain. All the curves have a maximum at $\tau^5 \approx 11.1$ but with increasing plastic strain the center of gravity of the distribution curves shifts to a higher ζ-value. The plastic strain dependence of the mean strain accommodation parameter $\bar{\zeta}$ is shown in Fig. 7(b) for deformation temperatures of 760 and 800°C. At both temperatures, a strong shift of the distribution curves to higher ζ-values occurs at the onset of plastic deformation and is followed by a saturation at higher plastic strains.

The slip-plane normals of numerous dislocations were calculated according to $\vec{n} = \vec{l} \times \vec{b}_\parallel$, where $\vec{l}$ is the line direction of a dislocation segment. It is found that slip occurs on low indexed planes. At a 2-fold [0/0 0/0 0/2] compression direction, the most frequently observed slip systems consist of a 5-fold (0/0 1/0 0/1) slip plane with a 2-fold $\langle 1/0\ \bar{1}/\bar{1}\ 0/1 \rangle$ slip direction and a 5-fold (0/1 0/0 1/0) slip plane with a 2-fold $\langle 0/\bar{1}\ 1/0\ 1/1 \rangle$ slip direction, both having a Schmid factor of 0.43. Less frequently, other slip systems with 2-fold and 3-fold slip planes, having a smaller Schmid factor, are found.

5. In-situ studies

Dislocation motion and interaction phenomena under applied stress can be observed directly by in-situ tensile experiments in a high-voltage electron micro-

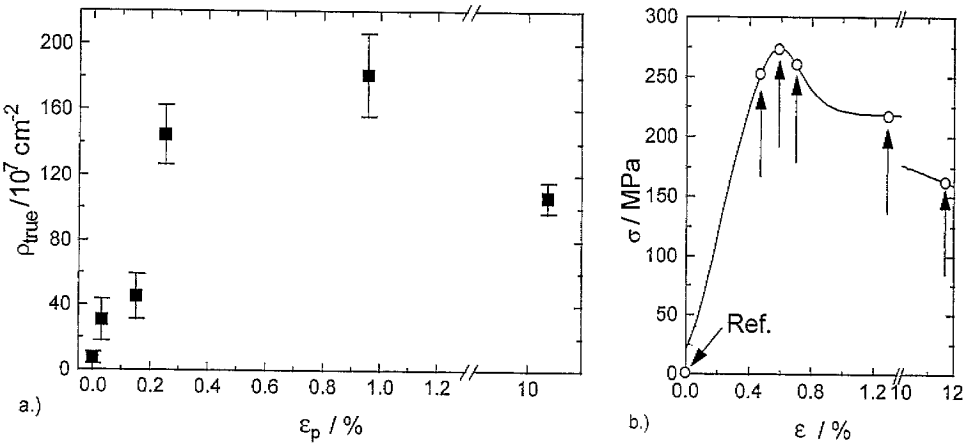

Fig. 6. (a) Dependence of the dislocation density ρ on plastic strain ε_p at 760°C. Note the axis break. (b) Corresponding stages of deformation marked in a stress–strain curve.

scope. Most experiments were performed at 750°C. Experimental details are described elsewhere [21,37].

Fig. 8 shows dislocations (black arrows) moving through an undeformed specimen area. The dislocation lines are slightly bowed out due to friction at the specimen surfaces. The motion is viscous. It is found that dislocations leave behind a planar-fault contrast, which in some cases disappears after some time. The dislocations show a pronounced tendency to follow each other on the same slip trace. Weak repulsive interaction forces act between dislocations moving on neighbouring slip traces. No examples of the demobilization of moving dislocations by interaction processes of any kind could be observed. Moreover, interactions with sessile or slowly moving dislocations often catalyze cross-slip phenomena or multiplication processes. The planes of motion were identified as 3-fold and 5-fold type planes [22]. In the course of numerous experiments, some multiplication mechanisms and a dislocation source have been observed.

6. Discussion

A number of experimental observations can be interpreted directly in order to outline the deformation mechanism in icosahedral quasicrystals. Plastic deformation in the ductile temperature regime is based on thermally activated dislocation motion which mainly involves dislocations with 2-fold Burgers vectors. Dislocations move on low-indexed planes of the quasilattice. These are 5-fold, 2-fold and 3-fold planes which, in this order, also correspond to the densest planes in the Al–Pd–Mn structure.

The activation volume is about two orders of magnitude larger than $b_{\|}^3$ and is strongly stress-dependent. From this we conclude that the rate of plastic deformation is controlled by obstacles rather than by a diffusion mechanism. This is supported by the observation that the activation enthalpy is much larger than the enthalpy of self-diffusion in this material, which amounts to 1.99 eV [38]. However, the small absolute value of the order of 1 nm^3 found for the activation volume shows that the density of rate-controlling obstacles is high.

Measurements of thermodynamic activation parameters were reported by other workers on some poly-quasicrystalline icosahedral alloys. In poly-quasicrystalline Al–Pd–Mn [17], Al–Cu–Fe [15] and Al–Cu–Ru [16], comparable values were obtained. In particular, the activation enthalpy is always found to be extraordinarily large [16,17].

The further discussion is based on details of the atomic structure of icosahedral Al–Pd–Mn. The structure in physical space, in accordance with the deterministic structure models (Section 2.1), is found to consist of a hierarchical arrangement of clusters [39]. The smallest unit (~ 10 Å in diameter) is the so-called pseudo-Mackay cluster (PMC), which is an aggregate of 51 atoms arranged on centrosymmetric shells with icosahedral symmetry. PMCs are highly stable and govern several physical properties of icosahedral quasicrystals [39,40]. The fact that these clusters are hard objects was recently demonstrated by scanning tunneling microscopy of cleaved Al–Pd–Mn surfaces [41]. We propose that PMCs act as rate-controlling obstacles to dislocation motion in icosahedral quasicrystals [42].

Considering PMCs as rate-controlling obstacles, the activation volume can be roughly estimated as the product of the diameter and distance (~ 20 Å center to center) of the PMCs in Al–Pd–Mn. This yields a value of about 0.4 nm^3 which fits the value observed experimentally. The PMCs limit the mean dislocation velocity since they represent localized regions of higher mechanical strength. These must either be cut or circumvented by moving dislocations in the course of plastic defor-

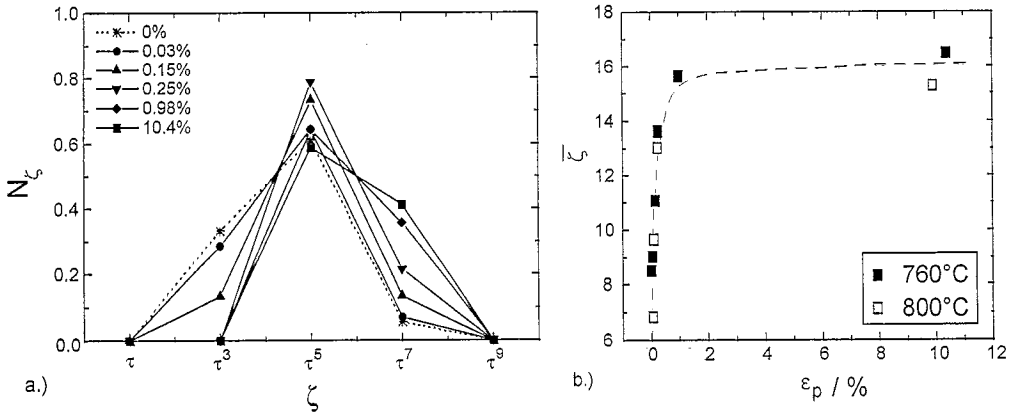

Fig. 7. (a) Normalized ζ-distribution curves of dislocations with 2-fold Burgers vectors for different values of plastic strain ($T = 760$°C). (b) Dependence of the mean ζ-value on plastic strain ε_p.

mation. Due to the high obstacle density, dislocation movement appears as a viscous motion through the cluster arrangement as is observed in the in-situ experiments. The process can be regarded as a generalized type of lattice friction, appearing on a larger length scale and without an underlying periodicity, which may be termed 'cluster friction'.

On the average, a decrease in the density of obstacles in the course of plastic deformation is expected. This is not only due to the destruction of obstacles by cut processes but also results directly from the introduction of structural and chemical disorder by moving dislocations. Due to the aperiodicity of the quasilattice, any shear is unavoidably connected with the introduction of matching-rule violations. Thus, in the wake of a moving dislocation a layer of high phason density is left behind. Since the cluster structure is characteristic of the ideal quasicrystal, the introduction of phason disorder on the average causes a reduction of obstacles. This means that the structure is weakened in the sense that dislocation motion becomes easier. Corresponding observations were made in the in-situ experiments, where dislocations distinctly tend to follow each other in the same traces and in molecular dynamics simulations of shear deformation of a model quasicrystal [23,24].

Fig. 8. Bright-field image of moving dislocations during an in-situ straining experiment in a high-voltage electron microscope at 750°C. Bar = 2 μm.

The disordering of the material is observed experimentally as an increase of the mean strain accommodation parameter with increasing plastic strain (Fig. 7). This corresponds to an average increase of the phason component of the Burgers vector and thus shows that phasons are introduced and accumulated in the material during plastic deformation. This is further corroborated by the high value of the activation enthalpy ΔH of about 7 eV. The physically relevant quantity determining the temperature dependence of the plastic strain rate is the Gibbs free energy ΔG [43], which is connected to the experimentally accessible activation enthalpy by the thermodynamic relation $\Delta G = \Delta H - T\,\Delta S$. Finite plastic strain rates at temperatures around 750°C, for which $kT \approx 0.09$ eV, cannot be obtained without postulating a substantial entropy contribution ΔS, which leads to a physically reasonable value of ΔG. The disordering concept allows part of the high activation enthalpy to be attributed to the energy increase associated with the phason strain introduced. On the other hand, the introduction of chemical and structural disorder induces a considerable increase in the entropy of the system. These contributions are suited to arrive at a Gibbs free energy of a few electron volts in order to allow thermally activated dislocation motion at the temperatures of our experiments.

However, if the material is weakened in the course of plastic deformation a reduced force is needed to maintain a given dislocation velocity. As a consequence, in experiments at constant strain rate this will lead to a decrease of the flow stress with increasing plastic strain.

Additionally, we observe a reduction of the dislocation density at higher strains. The dip tests, yielding low internal stresses, show that the influence of the decrease in dislocation density on the flow stress can only to a very small part be attributed to athermal processes. The average dislocation velocity, which has to increase in order to compensate for the decreasing density of mobile dislocations, is *not* accompanied by an increase of the flow stress. Therefore, the experimentally observed decrease of the flow stress is a consequence of the reduction of the friction stress, i.e., a substantial weakening of the structure as is expected from the cluster friction model.

In conclusion, we find that this qualitative model, which is ultimately a consequence of the specific icosahedral structure, can describe the observed deformation behavior appropriately and give an explanation for the most striking feature in quasicrystal plastic deformation, the work softening.

References

[1] D. Shechtman, I. Blech, D. Gratias, J.W. Cahn, Physical Review Letters 53 (1984) 1951.
[2] P. Sainfort, B. Dubost, Journal de Physique (Paris) 47 (1986) 321.
[3] A.P. Tsai, A. Inoue, T. Masumoto, Material Transactions of the Japanese Institute of Metals 29 (1988) 521.
[4] A.P. Tsai, A. Inoue, Y. Yokoyama, T. Masumoto, Philosophical Magazine Letters 61 (1990) 9.
[5] Y. Yokoyama, T. Miura, A.P. Tsai, A. Inoue, T. Masumoto, Material Transactions of the Japanese Institute of Metals 33 (1992) 97.
[6] M. Boudard, E. Bourgeat-Lami, M. de Boissieu, C. Janot, M. Durand-Charre, H. Klein, M. Audier, B. Hennion, Philosophical Magazine Letters 71 (1995) 11.
[7] H.S. Chen, C.H. Chen, A. Inoue, J.T. Krause, Physical Review B32 (1985) 1940.
[8] S.B. Bhaduri, J.A. Sekhar, Nature 327 (1987) 609.
[9] G.A.M. Reynolds, B. Golding, A.R. Kortan, J.M. Parsey Jr., Physical Review B41 (1990) 1194.
[10] R. Wittmann, K. Urban, M. Schandl, E. Hornbogen, Journal of Materials Research 6 (1991) 1165.
[11] Y. Yokoyama, A. Inoue, T. Masumoto, Material Transactions of the Japanese Institute of Metals 34 (1993) 135.
[12] Y. Amazit, M. Fischer, B. Perrin, A. Zarambowitch, M. De Boissieu, Europhysics Letters 25 (1994) 441.
[13] M. Feuerbacher, M. Weller, J. Diehl, K. Urban, Philosophical Magazine Letters 74 (1996) 81.
[14] S.S. Kang, J.M. Dubois, Philosophical Magazine A66 (1992) 151.
[15] L. Bresson, D. Gratias, Journal of Non-Crystalline Solids, 153/154 (1993) 468.
[16] T. Shibuya, T. Hashimoto, S. Takeuchi, Japanese Journal of Applied Physics 29 (1990) 349.
[17] S. Takeuchi, T. Hashimoto, Japanese Journal of Applied Physics 32 (1993) 2063.
[18] M. Wollgarten, M. Beyss, K. Urban, H. Liebertz, U. Köster, Physical Review Letters 71 (1993) 549.
[19] M. Feuerbacher, B. Baufeld, R. Rosenfeld, M. Bartsch, G. Hanke, M. Beyss, M. Wollgarten, U. Messerschmidt, K. Urban, Philosophical Magazine Letters 71 (1995) 91.
[20] R. Rosenfeld, M. Feuerbacher, B. Baufeld, M. Bartsch, M. Wollgarten, G. Hanke, M. Beyss, U. Messerschmidt, K. Urban, Philosophical Magazine Letters 72 (1995) 375.
[21] M. Wollgarten, M. Bartsch, U. Messerschmidt, M. Feuerbacher, R. Rosenfeld, M. Beyss, K. Urban, Philosophical Magazine Letters 71 (1995) 99.
[22] T.C. Lubensky, S. Ramaswamy, J. Toner, Physical Review B33 (1986) 7715.
[23] R. Mikulla, J. Roth, H.-R. Trebin, Philosophical Magazine B71 (1995) 981.
[24] R. Mikulla, J. Roth, H.-R. Trebin, Proceedings of the 5th International Conference on Quasicrystals, Avignon, France, 1995, World Scientific, Singapore, 1995, p. 298.
[25] M. Boudard, M. de Boissieu, C. Janot, G. Heger, C. Beeli, H.-U. Nissen, H. Vincent, R. Ibberson, M. Audier, J.M. Dubois, Journal of Phys. Condensed Matter 4 (1992) 10149.
[26] C. Janot, Quasicrystals, Clarendon Press, Oxford, 1994.
[27] A. Katz, M. Duneau, Journal de Physique (Paris) 47 (1986) 181.
[28] M. Wollgarten, K. Urban, in: F. Hippert, D. Gratias (Eds.), Lectures on Quasicrystals, Les Editions de Physique, Les Ulis, France, 1994, p. 535.
[29] J.E.S. Socolar, T.C. Lubensky, P.J. Steinhardt, Physical Review B34 (1986) 3345.
[30] J. Bohsung, H.-R.Trebin, in: M.V. Jaric (Ed.), Aperiodicity and Order, Academic Press, London, 1989, p. 183.
[31] M. Kléman, in: C. Janot, J.M. Dubois (Eds.), Quasicrystalline Materials, World Scientific, Singapore, 1988, p. 318.
[32] A. Katz, D. Gratias, in: F. Hippert, D. Gratias (Eds.), Lectures on Quasicrystals, Les Editions de Physique, Les Ulis, France, 1994, p. 187.
[33] M. Wollgarten, D. Gratias, Z. Zhang, K. Urban, Philosophical Magazine A64 (1991) 819.
[34] R. Wang, Y. Cheng, Materials Science Forum 22–24 (1987) 409.
[35] U.F. Kocks, A.S. Argon, M.F. Ashby, Thermodynamics and Kinetics of Slip, Pergamon Press, Oxford, 1975.
[36] J.W. Cahn, D. Shechtman, D. Gratias, Journal of Materials Research 1 (1986) 13.
[37] U. Messerschmidt, M. Bartsch, Ultramicroscopy 56 (1994) 163.
[38] T. Zumkley, H. Mehrer, K. Freitag, M. Wollgarten, N. Tamura, K. Urban, Physical Review B, 54 (1996) R6815.
[39] C. Janot, M. De Boissieu, Physical Review Letters 72 (1994) 1647.
[40] C. Janot, Physical Review B53 (1996) 181.
[41] P. Ebert, M. Feuerbacher, N. Tamura, M. Wollgarten, K. Urban, Physical Review Letters, 77 (1996) 3827.
[42] M. Feuerbacher, R. Rosenfeld, B. Baufeld, M. Bartsch, U. Messerschmidt, M. Wollgarten, K. Urban, Proceedings of the 5th International Conference on Quasicrystals, Avignon, France, 1995, World Scientific, Singapore, 1995, p. 714.
[43] G. Schöck, Physica Status Solidi 8 (1965) 499.